

Solution to Problem 1

a) Two voltage equations are:

$$L \frac{dI(t)}{dt} + M \frac{dI_s(t)}{dt} + RI = 0 \quad (S2.1a)$$

$$M \frac{dI(t)}{dt} + L_s \frac{dI_s(t)}{dt} = 0 \quad (S2.1b)$$

b) Solving for $I_s(t)$ from Eq. S2.1b, we obtain:

$$I_s(t) = -\frac{M}{L_s} I(t) + C \quad (S2.2)$$

Because $I_s(t=0) = 0$, $C = 0$, and because $I(t=0) = I(t=\infty) = 0$, $I_s(t) \neq 0$ only when $I(t) \neq 0$. That is, a “virgin” closed superconducting circuit cannot remain energized alone, with an external current source shut off.

Solution to Problem 2

For $r \gg \delta_d$, r_j of each dipole may be given in terms of r and θ :

$$r_1 \simeq r - \delta_d \sin \theta \quad (S4.1a)$$

$$r_2 \simeq r + \delta_d \cos \theta \quad (S4.1b)$$

$$r_3 \simeq r + \delta_d \sin \theta \quad (S4.1c)$$

$$r_4 \simeq r - \delta_d \cos \theta \quad (S4.1d)$$

With Eq. S4.1 into Eq. 2.51 for each dipole and ϑ_j expressed in terms of θ :

$$\vec{B}_1 \simeq \frac{r_d^2 \ell_d B_o}{2(r - \delta_d \sin \theta)^3} (-\cos \theta \vec{i}_r - \frac{1}{2} \sin \theta \vec{i}_\theta) \quad (S4.2a)$$

$$\vec{B}_2 \simeq \frac{r_d^2 \ell_d B_o}{2(r + \delta_d \cos \theta)^3} (\sin \theta \vec{i}_r - \frac{1}{2} \cos \theta \vec{i}_\theta) \quad (S4.2b)$$

$$\vec{B}_3 \simeq \frac{r_d^2 \ell_d B_o}{2(r + \delta_d \sin \theta)^3} (\cos \theta \vec{i}_r + \frac{1}{2} \sin \theta \vec{i}_\theta) \quad (S4.2c)$$

$$\vec{B}_4 \simeq \frac{r_d^2 \ell_d B_o}{2(r - \delta_d \cos \theta)^3} (-\sin \theta \vec{i}_r + \frac{1}{2} \cos \theta \vec{i}_\theta) \quad (S4.2d)$$

For $r \gg \delta_d$ the denominator of each term may be expanded; to 1st order in δ_d/r Eq. S4.2 becomes:

$$\vec{B}_1 \simeq \frac{r_d^2 \ell_d B_o}{2r^3} \left[1 + 3 \left(\frac{\delta_d}{r} \right) \sin \theta \right] (-\cos \theta \vec{i}_r - \frac{1}{2} \sin \theta \vec{i}_\theta) \quad (S4.3a)$$

$$\vec{B}_2 \simeq \frac{r_d^2 \ell_d B_o}{2r^3} \left[1 - 3 \left(\frac{\delta_d}{r} \right) \cos \theta \right] (\sin \theta \vec{i}_r - \frac{1}{2} \cos \theta \vec{i}_\theta) \quad (S4.3b)$$

$$\vec{B}_3 \simeq \frac{r_d^2 \ell_d B_o}{2r^3} \left[1 - 3 \left(\frac{\delta_d}{r} \right) \sin \theta \right] (\cos \theta \vec{i}_r + \frac{1}{2} \sin \theta \vec{i}_\theta) \quad (S4.3c)$$

$$\vec{B}_4 \simeq \frac{r_d^2 \ell_d B_o}{2r^3} \left[1 + 3 \left(\frac{\delta_d}{r} \right) \cos \theta \right] (-\sin \theta \vec{i}_r + \frac{1}{2} \cos \theta \vec{i}_\theta) \quad (S4.3d)$$

Combining each field given by Eq. S4.3, we obtain:

$$\vec{B} = \vec{B}_1 + \vec{B}_2 + \vec{B}_3 + \vec{B}_4 \simeq \frac{3r_d^2 \ell_d B_o \delta_d}{r^4} (-\sin 2\theta \vec{i}_r + \frac{1}{2} \cos 2\theta \vec{i}_\theta) \quad (2.52)$$

Note that $|\vec{B}|$ decreases $\propto 1/r^4$ rather than $\propto 1/r^3$, as would a single dipole.

Solution to Problem 3

a) The centripetal force, \vec{F}_{cp} , on a circulating proton (mass M_p) is balanced by the Lorentz force, \vec{F}_L . The direction of B_z is chosen to make F_L point radially inward because F_{cp} always points radially outward. The two forces are given by:

$$\vec{F}_{cp} = \frac{M_p v^2}{R_a} \vec{i}_r \simeq \frac{M_p c^2}{R_a} \vec{i}_r = \frac{E_p}{R_a} \vec{i}_r \quad (S12.1a)$$

$$\vec{F}_L = -qcB_z \vec{i}_r \quad (S12.1b)$$

Solving for R_a from $\vec{F}_{cp} + \vec{F}_L = 0$, we obtain:

$$R_a = \frac{E_p}{qcB_z} \quad (S12.2)$$

From Eq. S12.2, we have:

$$\begin{aligned} R_a &= \frac{(1.6 \times 10^{-19} \text{ J/eV})(7 \times 10^{12} \text{ eV})}{(1.6 \times 10^{-19} \text{ C})(3 \times 10^8 \text{ m/s})(8.3 \text{ T})} \\ &\simeq 2.81 \times 10^3 \text{ m} \simeq 2.8 \text{ km} \end{aligned}$$

This is less than the actual radius of LHC, which is slightly over 4 km. Note that in the above computation it is assumed that the entire ring is occupied by dipoles; in fact the occupancy rate for the dipoles is $\sim 60\%$ —quadrupoles, detector magnets occupy most of the rest. The average dipole field along the LHC ring is thus $\sim 5 \text{ T}$, leading to a computed radius of $\sim 4 \text{ km}$. Of course, a dipole field of $B_z = 15 \text{ T}$, for example, will nearly halve the ring diameter; superconducting dipole magnets with a field in the range 10–16 T are not out of the question [3.54–3.56].

b) The proton mass M_p , traveling at speed v , is related to its rest mass, M_{p_0} ($1.67 \times 10^{-27} \text{ kg}$), by:

$$M_p = \frac{M_{p_0}}{\sqrt{1 - \left(\frac{v}{c}\right)^2}} = \frac{E_p}{c^2} \quad (S12.3)$$

Solving for v/c from Eq. S12.3, we have:

$$\frac{v}{c} = \sqrt{1 - \frac{M_{p_0}^2 c^4}{E_p^2}} \quad (S12.4)$$

Because v/c is very close to 1, Eq. S12.4 may be approximated by:

$$\begin{aligned} \frac{v}{c} &\simeq 1 - \frac{M_{p_0}^2 c^4}{2E_p^2} = 1 - \frac{(1.67 \times 10^{-27} \text{ kg})^2 (3 \times 10^8 \text{ m/s})^4}{2(1.6 \times 10^{-19} \text{ J/eV})^2 (7 \times 10^{12} \text{ eV})^2} \\ &\simeq 1 - 9 \times 10^{-9} \end{aligned}$$

That is, the proton velocity is within nine parts per billion of the speed of light.

Solution to Problem 4

a) Because of symmetry about $x = 0$, we shall consider only one half of the slab, between $x = 0$ and $x = a$. As illustrated in Fig. 5.18, the solid line corresponds to $H_{s1}(x)$, which gives the initial field distribution within the slab, with $J = J_c$. The dotted line corresponds to $H_{s2}(x)$ for the slab carrying $J_c - |\Delta J_c|$. Note that the field at the surface is H_e in both cases. We thus have:

$$H_{s1}(x) = H_e + J_c(x - a) \quad (S2.1a)$$

$$H_{s2}(x) = H_e + (J_c - |\Delta J_c|)(x - a) \quad (S2.1b)$$

Because there is a change in magnetic field within the slab, an electric field \vec{E} is generated, which from Faraday's law of induction is given by:

$$\oint_C \vec{E} \cdot d\vec{s} = -\mu_o \int_S \frac{\Delta H_s(x) \vec{i}_y \cdot d\vec{A}}{\Delta t} \quad (S2.2)$$

From symmetry we have $\vec{E}(x = 0) = 0$ and \vec{E} points in the z -direction. $\Delta H_s(x)$ is given by:

$$\begin{aligned} \Delta H_s(x) &= H_{s2}(x) - H_{s1}(x) \\ &= |\Delta J_c|(a - x) \end{aligned} \quad (S2.3)$$

Combining Eqs. S2.2 and S2.3, we obtain:

$$\begin{aligned} E_z(x) &= \mu_o \frac{|\Delta J_c|}{\Delta t} \int_0^x (a - x) dx \\ &= \mu_o \frac{|\Delta J_c|}{\Delta t} \left(ax - \frac{x^2}{2} \right) \end{aligned} \quad (S2.4)$$

Dissipation power density, $p(x)$, is given by $E_z(x)J_c$; the total energy density per unit length dissipated in the slab or per unit slab surface area in the y - z plane, \mathcal{E}_ϕ [J/m²], is given by:

$$\begin{aligned} \mathcal{E}_\phi &= \int_0^a p(x) \Delta t dx \\ &= \mu_o J_c |\Delta J_c| \int_0^a \left(ax - \frac{x^2}{2} \right) dx = \frac{\mu_o J_c |\Delta J_c| a^3}{3} \end{aligned} \quad (S2.5)$$

The average dissipation energy density, e_ϕ , is given by \mathcal{E}_ϕ/a :

$$e_\phi = \frac{\mu_o J_c |\Delta J_c| a^2}{3} \quad (5.37)$$

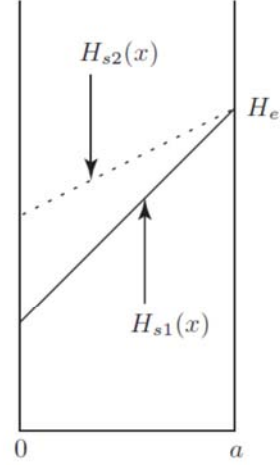


Fig. 5.18 Field profiles.

b) The Poynting energy flux $[J/m^2]$ in the y - z plane into the slab (in the $-x$ -direction) at $x = a$ is equal to the change in magnetic energy storage flux ΔE_m $[J/m^2]$ and dissipation energy flux \mathcal{E}_ϕ in the slab. Thus:

$$\int S_x(a) dt = \Delta E_m + \mathcal{E}_\phi \quad (S2.6)$$

We can verify the direction of \vec{S} by computing $\vec{S} = \vec{E} \times \vec{H}$ at $x = a$. At $x = a$, $\vec{H} = H_e \vec{i}_y$; from $E_z(x)$ derived in Eq. S2.4:

$$E_z(a) = \mu_o \frac{|\Delta J_c| a^2}{2\Delta t} \quad (S2.7)$$

Thus:

$$\vec{S}(a) = \mu_o \frac{|\Delta J_c| a^2}{2\Delta t} \vec{i}_z \times H_e \vec{i}_y = -\mu_o \frac{H_e |\Delta J_c| a^2}{2\Delta t} \vec{i}_x \quad (S2.8)$$

As expected, $\vec{S}(a)$ points in the $-x$ -direction; energy indeed flows into the slab. Thus:

$$\int S_x(a) dt = \mu_o \frac{H_e |\Delta J_c| a^2}{2} \quad (S2.9)$$

The difference in magnetic energy flux ΔE_m in the slab is given by:

$$\begin{aligned} \Delta E_m &= \frac{\mu_o}{2} \int_0^a [H_{s2}^2(x) - H_{s1}^2(x)] dx \\ &= \frac{\mu_o}{2} \int_0^a \{ [H_e + (J_c - |\Delta J_c|)(x - a)]^2 - [H_e + J_c(x - a)]^2 \} dx \\ &= \frac{\mu_o}{2} \int_0^a [-2H_e |\Delta J_c| (x - a) - 2J_c |\Delta J_c| (x - a)^2 + |\Delta J_c|^2 (x - a)^2] dx \end{aligned} \quad (S2.10)$$

Neglecting the $|\Delta J_c|^2$ term in the above integral, we obtain:

$$\Delta E_m = \mu_o \left(\frac{H_e |\Delta J_c| a^2}{2} - \frac{J_c |\Delta J_c| a^3}{3} \right) \quad (S2.11)$$

From Eq. S2.6, we have:

$$\mathcal{E}_\phi = \int S_x(a) dt - \Delta E_m \quad (S2.12)$$

Combining Eqs. S2.9, S2.11, and S2.12, we obtain:

$$\begin{aligned} \mathcal{E}_\phi &= \mu_o \frac{H_e |\Delta J_c| a^2}{2} - \mu_o \left(\frac{H_e |\Delta J_c| a^2}{2} - \frac{J_c |\Delta J_c| a^3}{3} \right) \\ &= \mu_o \frac{J_c |\Delta J_c| a^3}{3} \end{aligned} \quad (S2.13)$$

Equation S2.13 leads directly to Eq. 5.37:

$$e_\phi = \frac{\mathcal{E}_\phi}{a} = \frac{\mu_o J_c |\Delta J_c| a^2}{3} \quad (5.37)$$

c) As given by Eq. 5.38, $J_c(T)$ is a decreasing function of temperature. We thus have:

$$\Delta J_c = -J_{c_0} \left(\frac{\Delta T}{T_c - T_{op}} \right) \quad (5.39)$$

From Eq. 5.39, we have:

$$|\Delta J_c| = \frac{J_{c_0} \Delta T}{T_c - T_{op}} \quad (S2.14)$$

Replacing J_c with J_{c_0} in Eq. 5.37 and combining it with Eq. S2.14, we obtain:

$$e_\phi = \frac{\mu_0 J_{c_0}^2 \Delta T a^2}{3(T_c - T_{op})} \quad (S2.15)$$

Note that e_ϕ is proportional not only to ΔT but also, more importantly, to a^2 . Under adiabatic conditions, the dissipation energy density e_ϕ increases the superconductor's temperature by ΔT_s , given by:

$$\Delta T_s = \frac{e_\phi}{\tilde{C}_s} > 0 \quad (S2.16)$$

\tilde{C}_s is the superconductor's average heat capacity [J/m³K] in the temperature range from T_{op} to T_c . Combining Eqs. S2.15 and S2.16, and requiring $\Delta T_s < \Delta T$ for thermal stability, we have:

$$\frac{\Delta T_s}{\Delta T} < \frac{\mu_0 J_{c_0}^2 a^2}{3\tilde{C}_s(T_c - T_{op})} \quad (S2.17)$$

For a given superconducting material and operating temperature, a is the only parameter that can be varied by the magnet designer to satisfy Eq. S2.17. That is, thermal stability can be satisfied only if the slab half-width a is less than the critical size a_c , given by:

$$a_c = \sqrt{\frac{3\tilde{C}_s(T_c - T_{op})}{\mu_0 J_{c_0}^2}} \quad (5.40)$$

Equation 5.40 is applied to compute approximate values of a_c for NbTi (LTS) operating at 4.2 K and YBCO (HTS) operating at 77.3 K. Table 5.3 lists approximate values of parameters appearing in Eq. 5.40 for both superconductors.

We may conclude that for a circular filament of NbTi, $a_c = 140 \mu\text{m}$ means a critical diameter of $\sim 300 \mu\text{m}$ (Eq. 5.29) and a coated YBCO tape of width 8 mm.

Table 5.3: Application of Eq. 5.40 to NbTi and YBCO

<i>Superconductor</i>	T_{op} [K]	T_c [K]	J_{c_0} [A/m ²]	\tilde{C}_s [J/m ³ K]	a_c [mm]
NbTi	4.2	9.8	2×10^9	6×10^3	0.14
YBCO	77.3	93	2×10^9	2×10^6	4

Solution to Problem 5

a) Note that Traces A and C are independent of field sweep rate and that the corresponding magnetization—an indication of filament diameter—is much greater for Trace A than that for Trace C. We therefore conclude that Trace A is for Conductor 3 (monofilament) and that Trace C is for Conductor 1 (ℓ_{p1}). That leaves Trace B for Conductor 2 (ℓ_{p2}). (Remember that each conductor has the same volume of NbTi superconductor, and thus its measured magnetization should be directly proportional to filament diameter.)

b) The ratio of magnetization width, $(M(H_e \uparrow) - M(H_e \downarrow))$ of Conductor 3 (monofilament, Trace A) to that of Conductor 1 (Trace C), is roughly 10 for $\mu_o H_e$ below ~ 1 T (10 kilo-oersted). Therefore, we conclude that the filament diameter ratio is roughly 10.

c) Because a field sweep-rate of 900 oersted/sec ($\mu_o \dot{H}_{0z} = 0.09$ T/s) makes the magnetization of Conductor 2 (Trace B₃) nearly equal to that of Conductor 3 (Trace A), we may conclude that this sweep rate makes Conductor 2's filament twist pitch length ℓ_{p2} critical. Thus from Eq. 5.44:

$$\ell_{p2} = 2 \sqrt{\frac{2\rho_{cu} J_c d_f}{\mu_o \dot{H}_{0z}}} \quad (S5.1)$$

With $\rho_{cu} = 2 \times 10^{-10}$ Ω m; $J_c d_f = 4 \times 10^4$ A/m; and $\mu_o \dot{H}_{0z} = 0.09$ T/s, we obtain:

$$\begin{aligned} \ell_{p2} &= 2 \sqrt{\frac{(2)(2 \times 10^{-10} \Omega \text{ m})(4 \times 10^4 \text{ A/m})}{0.09 \text{ T/s}}} \\ &= 2.7 \times 10^{-2} \text{ m} = 27 \text{ mm} \end{aligned}$$

This value is close enough to the actual twist pitch of 10 mm. Because the magnetization of Conductor 1 (Trace C) at a sweep rate of 320 oersted/sec is considerably smaller than that of Conductor 2 for the same field sweep rate, we conclude that ℓ_{p1} is significantly shorter than ℓ_{p2} .

Solution to Problem 6

a) From the definition of R_s and using Eq. 6.25a for V_s , we have:

$$R_s = \frac{V_s}{I_s} = \frac{V_c}{I_s} \left(\frac{I_s}{I_c} \right)^n = \frac{V_c}{I_c} \left(\frac{I_s}{I_c} \right)^{(n-1)} \quad (S3.1)$$

With $R_c = V_c/I_c$, Eq. S3.1 becomes:

$$R_s = R_c \left(\frac{I_s}{I_c} \right)^{(n-1)} \quad (6.26a)$$

R_{dif} represents the superconductor's differential resistance at I_s , hence:

$$R_{dif} = \frac{\partial V_s}{\partial I_s} = \frac{nV_c}{I_c} \left(\frac{I_s}{I_c} \right)^{(n-1)} \quad (S3.2)$$

$$R_{dif} = nR_c \left(\frac{I_s}{I_c} \right)^{(n-1)} \quad (6.26a)$$

The partial differentiation is performed in Eq. S3.2 because in realistic situations the temperature dependance of I_c , i.e., $I_c(T)$, must be included in the analysis in the range $I_s > I_c$, where the composite is expected to be heated, here above 77.3 K.

b) The circuit must satisfy the following current and voltage equations:

$$I_t = I_m + I_s \quad (S3.3a)$$

$$V_m = R_m I_m = V_s = V_c \left(\frac{I_s}{I_c} \right)^n \quad (S3.3b)$$

As an illustration, let us compute I_m for $I_t = 90$ A. From Eq. S3.3a, we have: $I_s = 90 \text{ A} - I_m$. Inserting this into Eq. S3.3b, we obtain:

$$3 \times 10^{-4} \Omega \times I_m [\text{A}] = 10^{-5} \text{ V} \left(\frac{90 \text{ A} - I_m [\text{A}]}{100 \text{ A}} \right)^{15} \quad (S3.3c)$$

From Eq. S3.3c: $I_m = 0.00686$ A and hence $I_s = 89.99314$ A.

The total power dissipation in the composite superconductor, P_{cd} , is given by:

$$P_{cd} = R_m I_m I_t = V_s I_t \quad (S3.4)$$

The Joule dissipation flux, g_{jcd} is given simply by P_{cd} divided by the composite's total cooling surface, here 10 cm^2 .

Table 6.5a gives a summary of solution to b).

Table 6.5a: Summary of Solution to b) ($n=15$)

I_t [A]	I_m [A]	I_s [A]	$R_m I_m$ [V]	P_{cd} [W]	g_{jcd} [W/cm ²]	R_{dif} [Ω]
90	0.00686	89.99314	2.06×10^{-6}	185×10^{-6}	18.5×10^{-6}	0.343×10^{-6}
100	0.0332	99.967	9.95×10^{-6}	995×10^{-6}	99.5×10^{-6}	1.49×10^{-6}
120	0.483	119.517	145×10^{-6}	17.4×10^{-3}	1.74×10^{-3}	18.2×10^{-6}
150	7.07	142.93	2.12×10^{-3}	318×10^{-3}	31.8×10^{-3}	223×10^{-6}
300	126.75	173.25	38.0×10^{-3}	11.4	1.14	3.29×10^{-3}
500	315.88	184.12	94.8×10^{-3}	47.4	4.74	7.72×10^{-3}

c) Even when the composite is well-cooled by boiling cryogen, its temperature must rise to transfer Joule dissipation to the cryogen. With liquid nitrogen boiling at 77.3 K, this rise, which increases with heat flux, can be as high as ~ 10 K in the nucleate boiling range. The most obvious temperature-dependent parameter in Eq. 6.25a is I_c , which decreases with increasing temperature; the temperature-dependence of n is not well-documented, LTS or HTS—in an analysis of this nature, we may assume n to be constant. In the equivalent circuit, R_m , if it is a matrix of pure metal, remains constant at low temperatures and increases nearly linearly with temperature beyond ~ 30 K. I_c on the other hand may be assumed to decrease linearly with T . The $(I_s/I_c)^n$ term thus increases sharply with temperature as does, consequently, Joule dissipation. Next, in **PROBLEM 6.4**, we will perform a circuit analysis in which I_c and R_m are T -dependent.

d) Results for $n=30$ are summarized in Table 6.5b.

e) Table 6.5b also gives a summary of results with $n=60$.

Note that for $I_t > I_c = 100$ A the smaller the n , the smaller are I_m , $R_m I_m = V_s(I_s)$, P_{cd} , g_{jcd} , and R_{dif} ; for $I_t < 100$ A, the opposite is true. This could pose practical problems in a real situation. For instance, at $I_t = 150$ A, $R_m I_m = 2.12$ mV for an $n=15$ composite, while it is 11.3 mV for an $n=60$ composite: clearly for detection of a resistive voltage, the $n=60$ composite is preferable to the $n=15$ composite.

Table 6.5b: Summary of Solution to d), and e)

I_t [A]	I_m [A]	I_s [A]	$R_m I_m$ [V]	P_{cd} [W]	g_{jcd} [W/cm ²]	R_{dif} [Ω]
$n=30$						
90	0.00141	89.9986	0.424×10^{-6}	38.1×10^{-6}	3.81×10^{-6}	0.127×10^{-6}
100	0.0330	99.967	9.90×10^{-6}	990×10^{-6}	99.0×10^{-6}	2.97×10^{-6}
120	3.37	116.63	1.01×10^{-3}	121×10^{-3}	12.1×10^{-3}	260×10^{-6}
150	25.27	124.73	7.58×10^{-3}	1.14	114×10^{-3}	1.82×10^{-3}
300	167.16	132.8	50.1×10^{-3}	15.0	1.50	11.32×10^{-3}
500	363.67	136.33	109×10^{-3}	54.6	5.46	24.0×10^{-3}
$n=60$						
90	0.00006	89.99994	0.018×10^{-6}	1.62×10^{-6}	0.162×10^{-6}	0.012×10^{-6}
100	0.0327	99.9673	9.81×10^{-6}	981×10^{-6}	98.1×10^{-6}	5.89×10^{-6}
120	10.02	109.98	3.01×10^{-3}	361×10^{-3}	36.1×10^{-3}	1.64×10^{-3}
150	37.57	112.43	11.3×10^{-3}	1.69	169×10^{-3}	6.02×10^{-3}
300	184.55	115.45	55.4×10^{-3}	16.6	1.66	28.8×10^{-3}
500	383.14	116.86	114.9×10^{-3}	57.5	5.75	59.0×10^{-3}

